Electronic Supplementary Material (ESI) for Physical Chemistry Chemical Physics.

Internal heavy atom effects in phenothiazinium dyes: Enhancement of intersystem crossing by vibronic spin-orbit coupling

(Electronic Supplementary Information)

Angela Rodriguez-Serrano,[†,‡] Vidisha Rai-Constapel,[§] Martha C. Daza,[†] Markus Doerr,[†,*] and Christel M. Marian[§,*]

[†]Grupo de Bioquímica Teórica, Universidad Industrial de Santander, Carrera 27, Calle 9, Bucaramanga, Colombia

[‡]Grupo de Fotodinámica Molecular, Departamento de Química, Universidad de los Andes, Carrera 1 No. 18A - 10, Bogotá, Colombia.

[§]Institute of Theoretical and Computational Chemistry, Heinrich Heine University of Düsseldorf, Universitätsstr. 1,D-40225 Düsseldorf, Germany

*E-mails: markusdoerr@gmx.de; and Christel.Marian@uni-duesseldorf.de

1. Details regarding the basis set choice in oxonine

Due to the difficulties in finding the $S_1(\pi_H\pi_L^*)$ state minimum in oxonine employing the TZVP basis set, the performance of the SV(P) and TZVPP basis sets was tested additionally. This electronic state is of main importance for the description of the ISC process in oxonine. The excitation energies obtained using the three basis sets at the respective ground state geometries of oxonine are listed in Table S1. A prominent shift of the vertical excitation energy upon increasing the number of polarization functions in the basis set is found for the S_3 and T_3 ($n_{H-4}\pi_L^*$) states (about 0.11 eV when going from the SV(P) to the TZVPP basis set). In the case of the $\pi\pi^*$ states, only minor energy shifts between 0.01 and 0.04 eV are observed. Since ISC from $S_1(\pi_H\pi_L^*)$ to $T_3(n_{H-4}\pi_L^*)$ state for oxonine is not expected to be efficient, we considered the SV(P) basis set to be a good choice for studying the electronic structure and ISC efficiencies. Hence, a comparison of the calculated DFT/MRCI/SV(P) vertical excitation energies of oxonine with those calculated for selenine and thionine using the DFT/MRCI/TZVP level of theory is considered reasonable.

The C_{2v} optimized structure of the $S_1(\pi_H\pi_L^*)$ state of oxonine with the TZVP basis set is found to be a second-order saddle point ($\nu_1 = i2041$ and $\nu_2 = i145$ cm^{-1}, $\Delta E_{DFT/MRCI} = 2.33$ eV) and optimizations using lower symmetry constraints yielded structures whose DFT/MRCI adiabatic energies are larger than the vertical energies. A one-dimensional cut in the direction of both imaginary modes indicates that again the C_{2v} geometry is favored at the DFT/MRCI level (see Figure S1(c-d)). This shows a poorer resemblance between the corresponding TD-B3LYP/TZVP and DFT/MRCI//TZVP potential energy surfaces (PESs) compared to the TD-B3LYP/SV(P) and DFT/MRCI//SV(P) PESs. At the TD-B3LYP/SV(P) level, the $S_1(\pi_H\pi_L^*)$ state is also a first-order saddle point characterized by a $i2475$ cm^{-1} B_1-symmetric vibration (see Figure S1(a)) which corresponds to a minimum at the DFT/MRCI level. To further confirm our choice of the SV(P) basis set, we optimized a C_{2v} symmetric geometry of the $S_1(\pi_H\pi_L^*)$ state of oxonine using the more polarized TZVPP basis set. As found when using the SV(P) basis set, at the TD-B3LYP/TZVPP PES the C_{2v} geometry corresponds to a first-order saddle point ($i1894$ cm^{-1}). Thus, we employed the C_{2v}-symmetric (TD-B3LYP/SV(P)) structure for the evaluation of the ISC rate constants where we replaced the imaginary vibrational frequency by a real value.

Table S1 Vertical excitation energies ($\Delta E_{(vac)}$, eV) of the low-lying singlet and triplet states of oxonine calculated at the DFT/MRCI level using SV(P), TZVP and TZVPP basis sets.

Electronic state	Electronic structure[a]	OXONINE		
		DFT/MRCI/SV(P)// B3LYP/SV(P)[b]	DFT/MRCI/TZVP// B3LYP/TZVP[b]	DFT/MRCI/TZVPP// B3LYP/TZVPP[b]
$S_0(1^1A_1)$	(93) Ground state			
$S_1(1^1B_1)$	(82) $\pi_H\pi_L^*$	2.39(0.998)	2.37(0.997)	2.41(0.996)
$S_2(2^1A_1)$	(80) $\pi_{H-1}\pi_L^*$	2.83(0.000)	2.82(0.000)	2.84(0.000)
$S_3(1^1B_2)$	(80) $n_{H-4}\pi_L^*$	3.16(0.003)	3.27(0.003)	3.27(0.002)
$S_4(3^1A_1)$	(48) $\pi_{H-2}\pi_L^*$ (25) $\pi_H\pi_L^*$ $\pi_H\pi_L^*$	3.64(0.028)	3.61(0.031)	3.63(0.028)
$S_5(2^1B_1)$	(73) $\pi_{H-3}\pi_L^*$	3.64(0.015)	3.61(0.015)	3.62(0.016)
$T_1(1^3B_1)$	(92) $\pi_H\pi_L^*$	1.61	1.59	1.59
$T_2(1^3A_1)$	(86) $\pi_{H-1}\pi_L^*$	2.49	2.49	2.53
$T_3(1^3B_2)$	(82) $n_{H-4}\pi_L^*$	2.80	2.90	2.92
$T_4(2^3A_1)$	(79) $\pi_{H-2}\pi_L^*$	3.13	3.13	3.18

[a]Dominant contributions at the DFT/MRCI/SV(P) level (percentage in parentheses). [b]The absorption oscillator strengths $f(r)$ are shown in parenthesis.

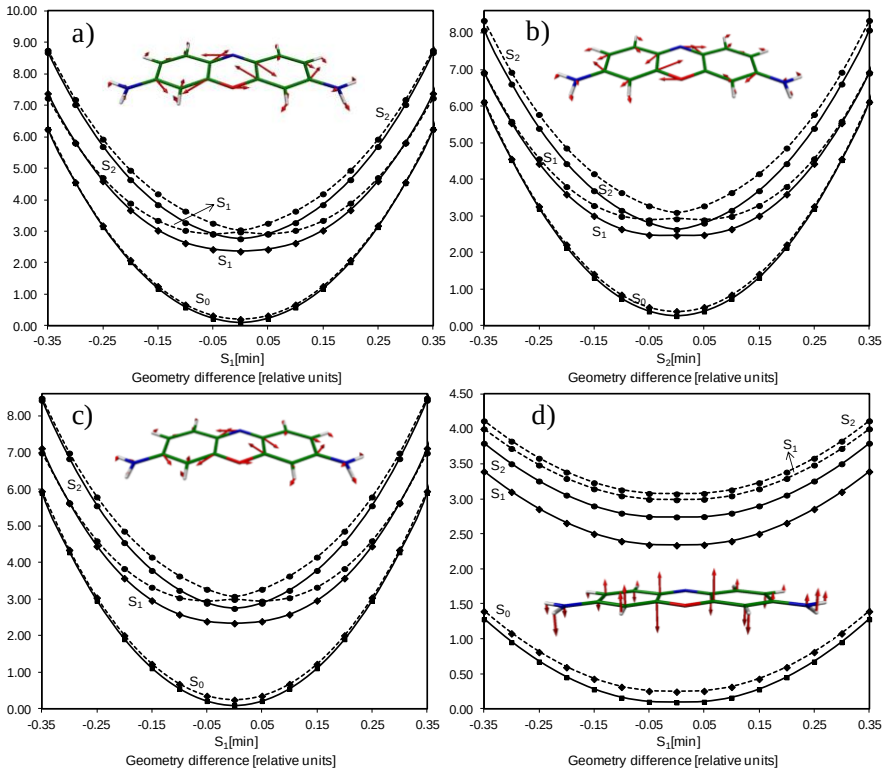

Figure S1 DFT/MRCI excitation energies calculated upon geometry distortions along the imaginary modes obtained at the S_1 and S_2 structures of oxonine. Bold lines refer to DFT/MRCI energies and dashed lines to those calculated with the B3LYP functional. a) $S_1(\pi_H\pi_L^*)$ geometry ($\nu_1(B_1) = i2475$ cm^{-1}), SV(P) basis set, b) $S_2(\pi_{H-1}\pi_L^*)$ geometry ($\nu_1(B_1) = i1342$ cm^{-1}), SV(P) basis set, c) $S_1(\pi_H\pi_L^*)$ geometry ($\nu_1(B_1) = i2041$ cm^{-1}), TZVP basis set and d) $S_1(\pi_H\pi_L^*)$ state ($\nu_2(A_2) = i145$ cm^{-1}), TZVP basis set.

2. TDDFT equilibrium structures of the ground and excited states of oxonine and selenine

The TDDFT equilibrium structures for the ground and excited states of oxonine and selenine are presented in Figure S2 and Figure S3, respectively. The computed electronic ground state minima of oxonine and selenine are all C_{2v} symmetric, in analogy to thionine. The main geometrical variation between the three dyes is found to be the central ring angle <C-X-C (where X = O, S, Se) and the C-X bond lengths. The presence of the selenium atom causes the C-Se bond (189 pm) to be longer than the corresponding bonds in thionine (C-S = 175 pm) and oxonine (C-O = 135 pm). Moreover, the computed minima of the S_1,T_1($\pi_H\pi_L$*) and S_2,T_2($\pi_{H-1}\pi_L$*) states of oxonine and selenine do not show significant geometrical variations in comparison to the ground state of each corresponding dye. These variations are presented in the following figures.

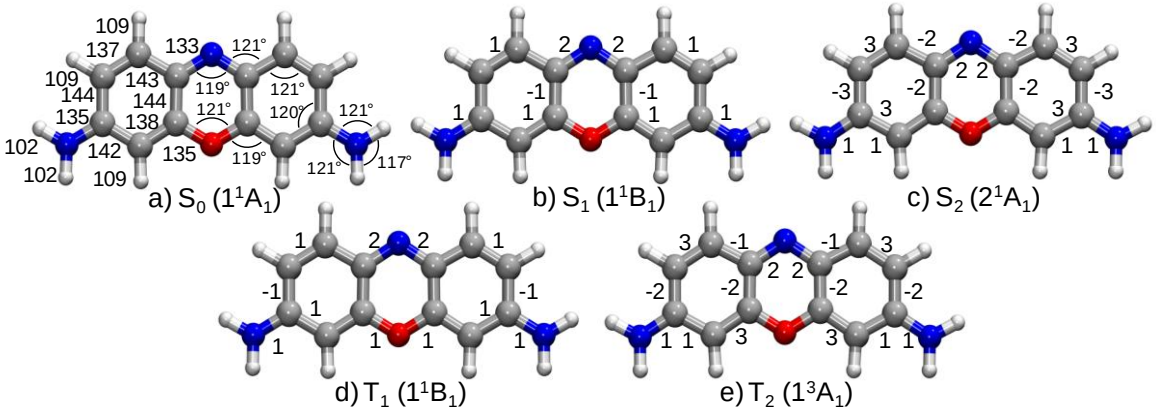

Figure S2. Computed (TD-)DFT equilibrium structures of the excited states of oxonine in comparison with the ground state (S_0) geometry. Numbers indicate bond lengths in pm (S_0 structure) and changes of bond lengths relative to the S_0 structure (all other structures). Bond angles are given in degrees.

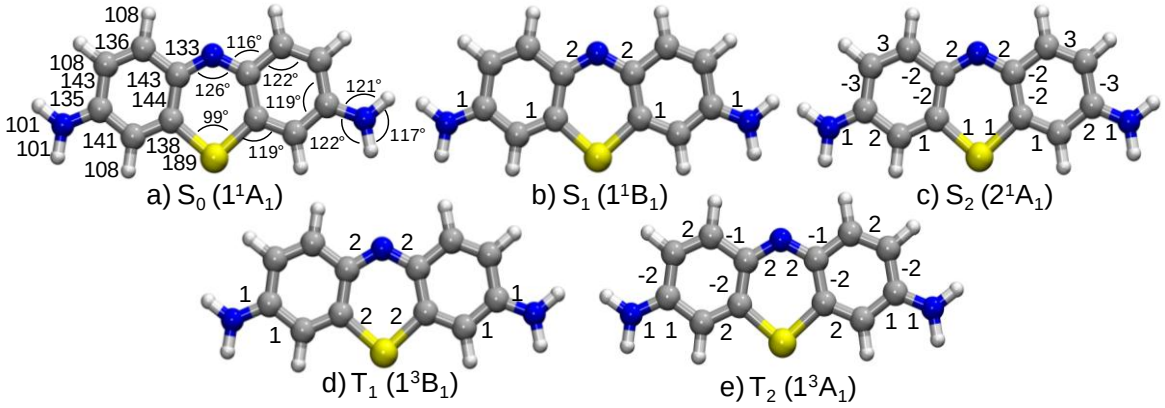

Figure S3. Computed (TD-)DFT equilibrium structures of excited states of selenine in comparison with the ground state (S_0) geometry. Numbers indicate bond lengths in pm (S_0 structure) and changes of bond lengths relative to the S_0 structure (all other structures). Bond angles and dihedrals are given in degrees.

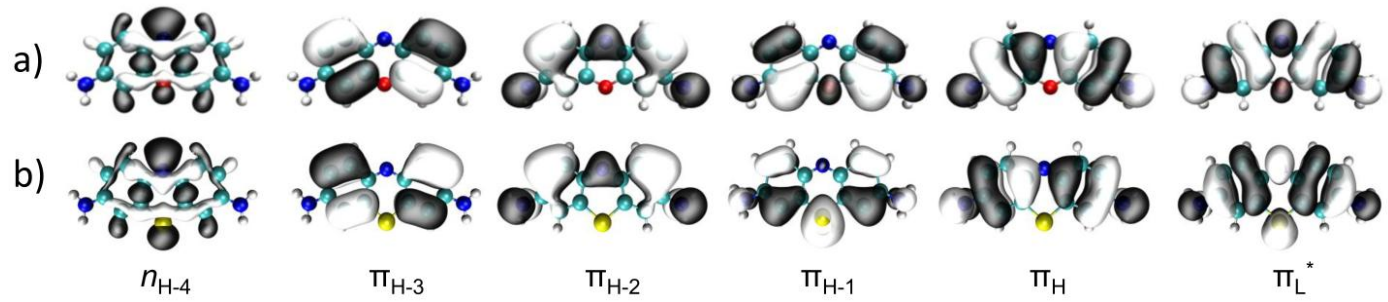

Figure S4. Frontier Kohn-Sham molecular orbitals computed at the ground state minimum of a) oxonine and b) selenine (isovalue 0.02).

3. TDDFT adiabatic energies at the computed excited state minima of oxonine and selenine

Table S2 Adiabatic TD-DFT excitation energies (eV) in vacuum (ΔE_{vac}^{ad}). Oscillator strengths for emission at the excited-state minima are listed in parentheses.

State	Character	Oxonine[b]		Selenine[c]	
		DC[a]	ΔE_{vac}^{ad}	DC[a]	ΔE_{vac}^{ad}
$S_1(1^1B_1)$	$\pi_H\pi_L^*$	96	2.82(0.588)	94	2.69(0.526)
$S_2(2^1A_1)$	$\pi_{H-1}\pi_L^*$	99	2.77(0.005)	98	2.47(0.023)
$T_1(1^3B_1)$	$\pi_H\pi_L^*$	99	1.45	99	1.46
$T_2(1^3A_1)$	$\pi_{H-1}\pi_L^*$	97	2.17	98	1.75

[a]Percentage of the dominant contributions. Adiabatic energies computed relative to the ground state energy at the ground state geometry at the [b]TD-B3LYP/SV(P) and [c]TD-B3LYP/TZVP theoretical levels.

4. Calculated intersystem crossing (ISC) rate constants using the time-dependent approach

4.1. OXONINE:

As described above, the optimized geometry for the $S_1(\pi_H\pi_L^*)$ state of oxonine at the TD-B3LYP/SV(P) level corresponds to a first-order saddle point (*i*2475 cm^{-1}). In the calculation of the ISC rate constants, this imaginary frequency was neglected assigning to the corresponding vibrational degree of freedom a positive harmonic frequency. Because the calculated values of the ISC rate constants are affected by the value of this frequency, we have evaluated the impact of this approximation on the computed ISC rate constants in Table S3.

Due to the large energy gap between the $S_1(\pi_H\pi_L^*)$ and $T_1(\pi_H\pi_L^*)$ states, the ISC rate constants through this channel are only slightly affected by the choice of the lowest vibrational harmonic frequency, the technical parameters and the temperature. The changes we obtained are below one order of magnitude. In contrast, the variation of the ISC rate constants is significant for the $S_1(\pi_H\pi_L^*) \rightsquigarrow T_2(\pi_{H-1}\pi_L^*)$ channel, due to the near-degeneracy between these electronic states. Here it is important to take the following into account:

i) The large imaginary frequency *i*2475 cm^{-1} corresponds to a B_1-symmetric vibration (Figure S1(a)). This mode is comprised by a backbone in-plane deformation of the system which is expected to occur at moderate vibrational frequencies. Therefore, we have evaluated the ISC rate constants substituting the imaginary frequency by wavenumbers of the lowest three B_1 modes of the $T_1(\pi_H\pi_L^*)$ state of oxonine (316.86, 391.81 and 509.24 cm^{-1}).

ii) Adiabatically, the $S_1(\pi_H\pi_L^*)$ state is located 174 cm^{-1} (0.022 eV) above the $T_2(\pi_{H-1}\pi_L^*)$ state (see Figure S5). Moreover, the ZPVE of the $T_2(\pi_{H-1}\pi_L^*)$ state is larger than that of the $S_1(\pi_H\pi_L^*)$ state (see Table 3 of the main text). Therefore, the choice of the vibrational frequency of the imaginary mode affects the relative position of the vibronic ground state of the $S_1(\pi_H\pi_L^*)$ state relative to that of the $T_2(\pi_{H-1}\pi_L^*)$ state. If it is chosen to be less than ~256 cm^{-1}, the vibronic ground state of the $S_1(\pi_H\pi_L^*)$ state lies below the vibronic ground state of the $T_2(\pi_{H-1}\pi_L^*)$ state. In this case the transition may not occur from the lowest vibrational level, but from some vibrationally excited level. For analyzing this effect on the computed ISC rate constants, we have also performed calculations employing a finite temperature (298 K) and using low frequency values for the imaginary frequency, such as 45, 50, 55, 60 and 65 cm^{-1}.

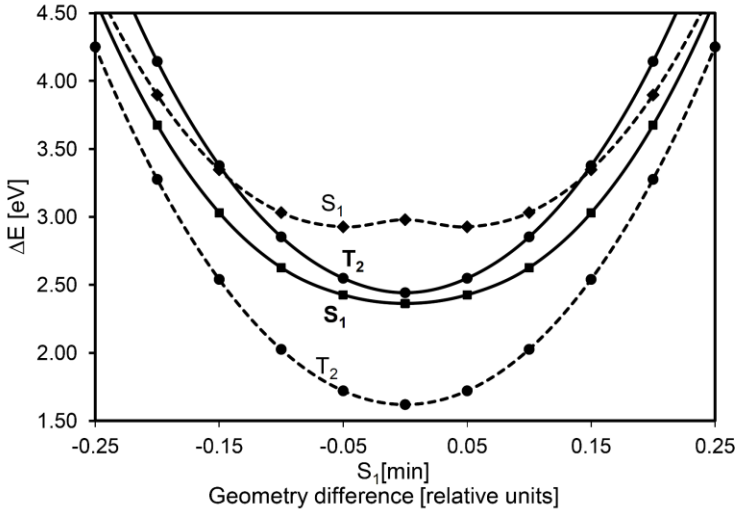

Figure S5 DFT/MRCI excitation energies of the $S_1(\pi_H\pi_L^*)$ and $T_2(\pi_{H-1}\pi_L^*)$ states calculated upon geometry distortions along the imaginary mode ($\nu_1(B_1) = i2475$ cm^{-1}) obtained at the optimized B3LYP/SV(P) geometry of the $S_1(\pi_H\pi_L^*)$ state of oxonine. Bold lines refer to DFT/MRCI energies and dashed lines to those calculated with the B3LYP functional.

In vacuum, the ISC rate constants for the $S_1(\pi_H\pi_L^*) \rightsquigarrow T_2(\pi_{H-1}\pi_L^*)$ channel (ΔE^{ad}= 0.02 eV) are calculated to be of the order of 10^8 s^{-1} (see Table S3) when the imaginary frequency is substituted by moderate frequency values (316.86, 391.81 and 509.24 cm^{-1}). The computed ISC rates for the same channel substituting the imaginary frequency by low frequencies (45, 50, 55, 60 and 65 cm^{-1}) are one order of magnitude smaller (10^7 s^{-1}). When hydration effects are accounted in the DFT/MRCI adiabatic excitation energies (ΔE^{ad}= -0.09 eV), the calculated ISC rate constants for this channel are two orders of magnitude below those calculated in vacuum for both situations. The calculated rate constants using low frequency values are computed to be one order of magnitude (10^5 s^{-1}) lower than when substituting the imaginary frequency by moderate frequencies (10^6 s^{-1}). Because of these variations and the reasoning explained above, we can only predict that the order of magnitude of the ISC rate constants for this transition is 10^7-10^8 s^{-1} in the gas phase and 10^5-10^6 s^{-1} in aqueous solution.

Table S3 Calculated rate constants $k_{ISC}(s^{-1})$ of oxonine for the $S_1 \rightsquigarrow T_i$ (i = 1,2) channels within the time-dependent approach. Other columns: adiabatic energy difference (ΔE^{ad}, eV), time interval (t, fs), number of points ($\#_{points}$) and damping factor (η, cm^{-1})

Channel	ΔE^{ad}	η	t	$\#_{points}$	k_{ISC}
Tests performed substituting the imaginary frequency at the S_1 state by ν_1 = 316.86 cm^{-1}					
$S_1 \rightsquigarrow T_1$	0.74	10	30000	900000	2.01×10^{6}
		10	50000	1500000	8.18×10^{5}
	0.81	10	30000	900000	1.05×10^{6}
		10	50000	1500000	1.33×10^{6}
$S_1 \rightsquigarrow T_2$	0.02[b]	10	30000	900000	1.43×10^{8}
		10	50000	1500000	1.42×10^{8}
	-0.09[a,b]	10	30000	900000	3.58×10^{6}
		10	50000	1500000	3.58×10^{6}
Tests performed substituting the imaginary frequency at the S_1 state by ν_1 = 391.81 cm^{-1}					
$S_1 \rightsquigarrow T_1$	0.74	10	30000	900000	6.21×10^{4}
		10	100000	3000000	2.55×10^{5}
	0.81	10	100000	3000000	1.25×10^{5}
		10	200000	6000000	1.30×10^{5}
$S_1 \rightsquigarrow T_2$	0.02[b]	10	30000	900000	1.11×10^{8}
		10	50000	1500000	1.12×10^{8}
	-0.09[a,b]	10	30000	900000	4.51×10^{6}
		10	50000	1500000	4.49×10^{6}
Tests performed substituting the imaginary frequency at the S_1 state by ν_1 = 509.24 cm^{-1}					
$S_1 \rightsquigarrow T_1$	0.74	10	100000	3000000	1.65×10^{5}
		10	200000	6000000	1.01×10^{5}
	0.81	10	30000	900000	2.53×10^{5}
		10	100000	3000000	5.07×10^{4}
		10	200000	6000000	7.33×10^{4}
$S_1 \rightsquigarrow T_2$	0.02[b]	10	30000	900000	1.39×10^{8}
		10	50000	1500000	1.40×10^{8}
	-0.09[a,b]	10	30000	900000	7.10×10^{6}
		10	50000	1500000	7.11×10^{6}
Tests performed substituting the imaginary frequency at the S_1 state by ν_1 = 45 cm^{-1}					
$S_1 \rightsquigarrow T_1$	0.74	1	30000	900000	5.85×10^{5}
		1	50000	1500000	5.85×10^{5}
		1	500000	15000000	5.85×10^{5}
		10	30000	900000	8.95×10^{5}
		10	300000	9000000	8.95×10^{5}
		10	500000	15000000	8.95×10^{5}
	0.81[a]	1	30000	900000	1.59×10^{6}
		1	50000	1500000	1.59×10^{6}
		10	30000	900000	1.88×10^{6}
		10	50000	1500000	1.88×10^{6}
$S_1 \rightsquigarrow T_2$	0.02[b]	10	3000	30000	1.24×10^{7}
		10	30000	300000	1.24×10^{7}
Tests performed substituting the imaginary frequency at the S_1 state by ν_1 = 50 cm^{-1}					
$S_1 \rightsquigarrow T_1$	0.74	10	30000	900000	1.27×10^{6}
		10	100000	3000000	1.78×10^{5}
	0.81[a]	10	30000	900000	6.90×10^{5}
		10	50000	1500000	2.66×10^{6}
$S_1 \rightsquigarrow T_2$	0.02[b]	10	30000	900000	1.45×10^{7}
		10	50000	1500000	1.45×10^{7}
	-0.09[a,b]	10	30000	900000	4.70×10^{5}
		10	50000	1500000	4.71×10^{5}
Tests performed substituting the imaginary frequency at the S_1 state by ν_1 = 55 cm^{-1}					
$S_1 \rightsquigarrow T_1$	0.74	10	30000	900000	1.22×10^{6}
		10	50000	1500000	6.73×10^{5}
	0.81[a]	10	30000	900000	1.51×10^{5}
		10	50000	1500000	5.54×10^{5}
$S_1 \rightsquigarrow T_2$	0.02[b]	10	30000	900000	1.72×10^{7}
		10	50000	1500000	1.71×10^{7}

Channel	ΔE^{ad}	η	t	$\#_{points}$	k_{ISC}
	-0.09[a,b]	10	30000	900000	5.24×10^{5}
		10	50000	1500000	5.25×10^{5}
Tests performed substituting the imaginary frequency at the S_1 state by ν_1 = 60 cm^{-1}					
$S_1 \rightsquigarrow T_1$	0.74	10	30000	900000	9.49×10^{5}
		10	50000	1500000	1.44×10^{6}
	0.81[a]	10	30000	900000	4.92×10^{6}
		10	50000	1500000	6.93×10^{6}
$S_1 \rightsquigarrow T_2$	0.02[b]	10	30000	900000	1.79×10^{7}
		10	50000	1500000	1.80×10^{7}
	-0.09[a,b]	10	30000	900000	5.88×10^{5}
		10	50000	1500000	5.90×10^{5}
Tests performed substituting the imaginary frequency at the S_1 state by ν_1 = 65 cm^{-1}					
$S_1 \rightsquigarrow T_1$	0.74	10	30000	900000	7.84×10^{5}
		10	50000	1500000	7.79×10^{5}
	0.81[a]	10	30000	900000	9.03×10^{5}
		10	50000	1500000	1.46×10^{6}
$S_1 \rightsquigarrow T_2$	0.02[b]	10	30000	900000	1.84×10^{7}
		10	50000	1500000	1.85×10^{7}
	-0.09[a,b]	10	30000	900000	6.38×10^{5}
		10	50000	1500000	6.37×10^{5}

[a]Rate constants calculated: applying spectroscopic solvation shifts from model $OXH^{+}3Wa$. [b]Rate computed at 298K

4.2. THIONINE:

Table S4 Calculated rate constants $k_{ISC}(s^{-1})$ of thionine for the $S_1 \rightsquigarrow T_i$ (i = 1,2) channels within the time-dependent approach. Other columns: adiabatic energy difference (ΔE^{ad}, eV), time interval (t, fs), number of points ($\#_{points}$) and damping factor (η, cm^{-1})

Channel	ΔE^{ad}	η	t	$\#_{points}$	$k_{ISC'}$
$S_1 \rightsquigarrow T_1$	0.64	0.10	30000	900000	3.72×10^{5}
		0.10	50000	1500000	1.83×10^{6}
		0.10	100000	3000000	8.79×10^{5}
		0.10	300000	9000000	1.08×10^{6}
		1	30000	900000	3.40×10^{6}
		1	50000	1500000	3.40×10^{6}
		1	100000	3000000	3.40×10^{6}
		1	300000	9000000	3.40×10^{6}
		10	30000	900000	3.57×10^{6}
		10	50000	1500000	3.57×10^{6}
		10	100000	3000000	3.57×10^{6}
		10	300000	9000000	3.57×10^{6}
	0.68[a]	0.10	30000	900000	6.43×10^{6}
		0.10	50000	1500000	4.44×10^{6}
		0.10	100000	3000000	3.48×10^{6}
		0.10	300000	9000000	3.15×10^{6}
		1	30000	900000	3.54×10^{6}
		1	50000	1500000	3.54×10^{6}
		1	100000	3000000	3.54×10^{6}
		1	300000	9000000	3.54×10^{6}
		10	30000	900000	2.52×10^{6}
		10	50000	1500000	2.52×10^{6}
		10	100000	3000000	2.52×10^{6}
		10	300000	9000000	2.52×10^{6}
$S_1 \rightsquigarrow T_2$	0.30	0.10	30000	900000	7.26×10^{8}
		0.10	50000	1500000	6.58×10^{8}
		0.10	100000	3000000	6.34×10^{8}
		0.10	300000	9000000	6.13×10^{8}
		0.10	500000	15000000	6.13×10^{8}
		1	30000	900000	6.45×10^{8}
		1	50000	1500000	6.45×10^{8}
		1	100000	3000000	6.45×10^{8}
		1	300000	9000000	6.45×10^{8}
		1	500000	15000000	6.45×10^{8}
		1	900000	27000000	6.45×10^{8}
		10	30000	900000	7.59×10^{8}
		10	50000	1500000	7.59×10^{8}
		10	100000	3000000	7.59×10^{8}
		10	300000	9000000	7.59×10^{8}
	0.21[a]	0.10	30000	900000	1.07×10^{9}
		0.10	50000	1500000	1.12×10^{9}
		0.10	300000	9000000	1.31×10^{9}
		1	30000	900000	1.07×10^{9}
		1	50000	1500000	1.07×10^{9}
		1	100000	3000000	1.07×10^{9}
		10	30000	900000	1.07×10^{9}
		10	50000	1500000	1.07×10^{9}
		10	100000	3000000	1.07×10^{9}

[a]Rate constants calculated: applying spectroscopic solvation shifts from model $TH^{+}3Wa$

4.3. SELENINE:

Table S5 Calculated rate constants $k_{ISC}^{TD}(s^{-1})$ of selenine for the $S_i \rightsquigarrow T_i$ (i = 1,2) channels within the time-dependent approach. Other columns: adiabatic energy difference (ΔE^{ad}, eV), time interval (t, fs), number of points ($\#_{points}$) and damping factor (η, cm^{-1})

Channel	ΔE^{ad}	η	t	$\#_{points}$	k_{ISC}
$S_1 \rightsquigarrow T_1$	0.62	1	30000	900000	3.84×10^{7}
		1	100000	3000000	3.84×10^{7}
		1	300000	9000000	3.84×10^{7}
		10	30000	900000	4.22×10^{7}
		10	100000	3000000	4.22×10^{7}
		10	300000	9000000	4.22×10^{7}
	0.68[a]	1	30000	900000	1.96×10^{7}
		1	100000	3000000	1.96×10^{7}
		1	300000	9000000	1.96×10^{7}
		10	30000	900000	2.59×10^{7}
		10	100000	3000000	2.59×10^{7}
		10	300000	9000000	2.59×10^{7}
$S_1 \rightsquigarrow T_2$	0.39	1	30000	900000	2.35×10^{10}
		1	100000	3000000	2.35×10^{10}
		1	300000	9000000	2.35×10^{10}
		10	30000	900000	1.66×10^{10}
		10	100000	3000000	1.66×10^{10}
		10	300000	9000000	1.66×10^{10}
	0.32[a]	1	30000	900000	2.57×10^{10}
		1	100000	3000000	2.57×10^{10}
		1	300000	9000000	2.57×10^{10}
		10	30000	900000	2.60×10^{10}
		10	100000	3000000	2.60×10^{10}
		10	300000	9000000	2.60×10^{10}
$S_2 \rightsquigarrow T_1$	0.58	1	30000	900000	9.93×10^{9}
		1	100000	3000000	9.93×10^{9}
		1	300000	9000000	9.93×10^{9}
		10	30000	900000	1.06×10^{10}
		10	100000	3000000	1.06×10^{10}
		10	300000	9000000	1.06×10^{10}
	0.69[a]	1	30000	900000	4.43×10^{9}
		1	100000	3000000	4.43×10^{9}
		1	300000	9000000	4.43×10^{9}
		10	30000	900000	4.65×10^{9}
		10	100000	3000000	4.65×10^{9}
		10	300000	9000000	4.65×10^{9}
$S_2 \rightsquigarrow T_2$	0.35	1	30000	900000	7.93×10^{8}
		1	100000	3000000	7.93×10^{8}
		1	300000	9000000	7.93×10^{8}
		10	30000	900000	1.04×10^{9}
		10	50000	1500000	1.04×10^{9}
		10	100000	3000000	1.04×10^{9}
		10	300000	9000000	1.04×10^{9}
	0.33[a]	1	30000	900000	1.44×10^{9}
		1	100000	3000000	1.44×10^{9}
		1	300000	9000000	1.44×10^{9}
		10	30000	900000	1.58×10^{9}
		10	50000	1500000	1.58×10^{9}
		10	100000	3000000	1.58×10^{9}
		10	300000	9000000	1.58×10^{9}

[a]Rate constants calculated: applying spectroscopic solvation shifts from model $SEH^{+}3Wa$